

Loss of Bardet–Biedl syndrome proteins causes defects in peripheral sensory innervation and function

Perciliz L. Tan^{*}, Travis Barr[†], Peter N. Inglis[‡], Norimasa Mitsuma^{*}, Susan M. Huang[§], Miguel A. Garcia-Gonzalez[¶], Brian A. Bradley[‡], Stephanie Coforio[†], Phillip J. Albrecht[†], Terry Watnick[¶], Gregory G. Germino[¶], Philip L. Beales[¶], Michael J. Caterina[§], Michel R. Leroux[‡], Frank L. Rice[†], and Nicholas Katsanis^{*,**}

^{*}McKusick–Nathans Institute of Genetic Medicine and Departments of [§]Biological Chemistry and [¶]Medicine, Johns Hopkins University School of Medicine, Baltimore, MD 21205; [†]Center for Neuropharmacology and Neuroscience, Albany Medical College, Albany, NY 12208; [‡]Department of Molecular Biology and Biochemistry, Simon Fraser University, Burnaby, BC, Canada V5 1S6; and [¶]Molecular Medicine Unit, Institute of Child Health, University College London, London WC1N 1EH, United Kingdom

Edited by Jeremy Nathans, Johns Hopkins University School of Medicine, Baltimore, MD, and approved September 7, 2007 (received for review July 13, 2007)

Reception and interpretation of environmental stimuli is critical for the survival of all organisms. Here, we show that the ablation of *BBS1* and *BBS4*, two genes mutated in Bardet–Biedl syndrome and that encode proteins that localize near the centrosomes of sensory neurons, leads to alterations of s.c. sensory innervation and trafficking of the thermosensory channel TRPV1 and the mechanosensory channel STOML3, with concomitant defects in peripheral thermosensation and mechanosensation. The thermosensory phenotype is recapitulated in *Caenorhabditis elegans*, because BBS mutants manifest deficient thermosensory responses at both physiological and nociceptive temperatures and defective trafficking of OSM-9, a polymodal sensory channel protein and a functional homolog of TRPV1 or TRPV4. Our findings suggest a hitherto unrecognized, but essential, role for mammalian basal body proteins in the acquisition of mechano- and thermosensory stimuli and highlight potentially clinical features of ciliopathies in humans.

basal bodies | cilia | thermosensation

The study of sensory organs in both vertebrates and invertebrates has revealed a role for cilia in chemosensation, mechanosensation, and photosensation. In *Drosophila*, chemosensation and mechanosensation rely specifically on neurons that are ciliated (1). Similarly, a role for cilia in chemosensation is well established in *Caenorhabditis elegans*, where mutants with compromised function or structure of cilia display defects in sensing odorants or differences in osmolarity (2–4). In mammals, odorant receptors localize to olfactory cilia (5), and the phototransduction apparatus of rod and cone cells in vertebrates localizes to the outer segment, a modified cilium (6). Finally, the kinocilium is essential for cochlear development and, thus, hearing because of its role in stereociliary bundle morphogenesis (7).

We and others have shown that loss-of-function mutations in genes underlying the pleiotropic Bardet–Biedl phenotype (8) cause sensory deficits that include vision loss, anosmia, and defective hearing (5, 7, 9, 10). All BBS proteins characterized to date localize near or within basal bodies and in cilia in both mammalian cells (11–13) and in *C. elegans* sensory neurons (14–16).

Here, we show that mammalian peripheral sensory neurons are ciliated and that mouse mutants with targeted loss-of-function mutations in either *Bbs1* or *Bbs4* exhibit thermosensory phenotypes characterized by significant increases in behavioral response latencies. These defects are unlikely to be caused by higher-order cortical or motor dysfunction but are accompanied by alterations in cutaneous sensory innervation and defective distribution of effector molecules in the sensory neuronal soma. These phenotypes are not unique to mammals, because nematode *bbs* mutants are also thermosensory-defective. Finally, humans with BBS also manifest some symptoms similar to the ones observed in mice, such as reduced temperature and vibration sensation. Our studies suggest a critical role of basal body and ciliary proteins for the function of

mammalian peripheral sensory neurons and the efficient transduction of extraorganismal stimuli.

Results

Dorsal Root Ganglia are Ciliated. In mammals, primary cilia have been observed in most postmitotic cells. However, they have never been reported in peripheral sensory neurons. Given that primary cilia perform critical functions in invertebrate sensory neurons, we investigated whether such cells might also be ciliated in mammals. Staining of dorsal root ganglia (DRG) sections with an antibody against the axonemal protein IFT88 (Polaris) (17) suggested the presence of cilia (data not shown), which was further supported by transmission electron microscopy (Fig. 1*A*, *F*, and *G*). To investigate this possibility more thoroughly, especially because DRG sections contain a heterogeneous population of cell types, we cultured DRG neurons from WT adult mice and stained cells with antibodies against a series of known axonemal proteins and anti-NeuN to discern neurons from other cell types. We observed specific staining along neuronal cilia for IFT88 (Fig. 1*B*) as well as IFT57 (data not shown). To confirm further that this was not a cross-reaction artifact, we transfected DRG cultures with a plasmid encoding an epitope-tagged (V5) axonemal protein, IFT81 (18). Costaining with an anti-V5 monoclonal antibody, as well as microtubule-associated protein 2 (MAP2; Fig. 1*C*), a neuronal dendritic marker, further supported the presence of a cilium on the soma of DRG neurons.

BBS Mutant Mice Have Thermo- and Mechanosensory-Defective Phenotypes. Null mutations in the BBS proteins have been associated with functional, but not structural, defects of the cilium both directly, as exemplified by retinal degeneration (9, 10) and anosmia (5), and indirectly, through the probable defective transmission of Wnt signal (7). We therefore wondered whether the presence of cilia in sensory neurons that innervate the skin might underscore other, hitherto unappreciated, sensory deficits in ciliopathy mutants.

First, to establish the presence of a cilium in the DRGs of BBS

Author contributions: T.B., P.N.I., and N.M. contributed equally to this work; P.L.T., T.B., P.N.I., N.M., S.M.H., P.L.B., M.J.C., M.R.L., F.L.R., and N.K. designed research; P.L.T., T.B., P.N.I., N.M., S.M.H., M.A.G.-G., B.A.B., S.C., P.L.B., and F.L.R. performed research; P.L.T., M.A.G.-G., B.A.B., T.W., G.G.G., and F.L.R. contributed new reagents/analytic tools; P.L.T., T.B., P.N.I., N.M., S.M.H., M.A.G.-G., B.A.B., S.C., P.J.A., T.W., G.G.G., P.L.B., M.J.C., M.R.L., F.L.R., and N.K. analyzed data; and P.L.T., T.B., P.N.I., S.M.H., M.A.G.-G., P.J.A., T.W., G.G.G., P.L.B., M.J.C., M.R.L., F.L.R., and N.K. wrote the paper.

The authors declare no conflict of interest.

This article is a PNAS Direct Submission.

Abbreviations: CGRP, calcitonin gene-related peptide; DRG, dorsal root ganglion; GHP, glabrous hind paw; PGP, protein gene product; BBS, Bardet–Biedl syndrome.

**To whom correspondence should be addressed. E-mail: katsanis@jhmi.edu.

This article contains supporting information online at www.pnas.org/cgi/content/full/0706618104/DC1.

© 2007 by The National Academy of Sciences of the USA

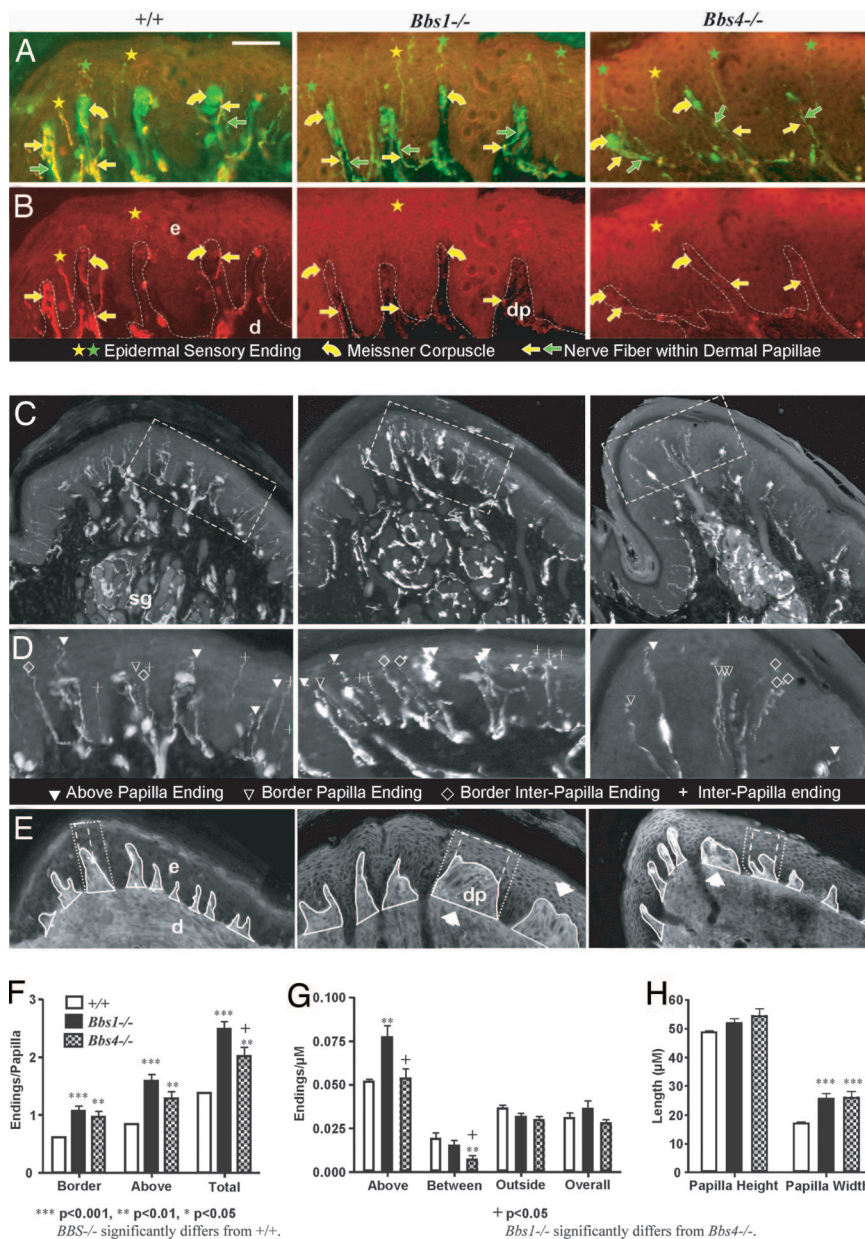


Fig. 3. Differences in epidermal structure and innervation in *Bbs*^{-/-} mice. (A and B) Images of distal pads from glabrous hind paws showing CGRP (red) with PGP (green) (A) and CGRP (B) immunolabeling alone. *Bbs*^{-/-} animals had reduced CGRP immunoreactivity in nerve fibers within dermal papillae (yellow arrows), whereas no differences were evident in the proportion of CGRP-positive epidermal endings (yellow stars). Green arrows and stars indicate PGP-positive dermal nerve fibers and epidermal endings, respectively. The epidermal–dermal border is indicated by a broken line. (C) Images of distal pads from WT and *Bbs*^{-/-} mice labeled for PGP 9.5. Innervation is evenly spaced throughout the epidermis of the WT pad but is concentrated at dermal papillae in *Bbs* mutants. (D) Close-up of the selected distal pad region illustrating the subjective classification of sensory endings based on their position in the epidermis relative to dermal papillae (between, above, or at the border of a papilla). Endings spanning multiple regions were labeled for each region they passed through (e.g., border interpapilla endings). (E) Images of distal pads labeled with anti-mouse Cy2 to delineate the dermal–epidermal border showing that *Bbs* mutants have large, misshaped dermal papillae (white arrowheads). Papillae (solid white lines) and examples of the subjectively determined regions above (dashed white lines) and at the border of a papilla (dotted white lines) are traced. (F–H) Quantification of epidermal innervation and dermal papilla structure conducted on tissue sections labeled with PGP 9.5 and mouse anti-Cy2. (F) Both *Bbs*^{-/-} mutants had significantly more endings above and at the border of papillae compared with WT, and *Bbs1*^{-/-} mice had significantly more total papillae endings than *Bbs4*^{-/-} mice. Total papillae endings were the sum of all endings that passed through the regions above or at the border of papillae. (G) *Bbs1*^{-/-} mice had a significantly greater density of endings above their papillae, and *Bbs4*^{-/-} mice had significantly fewer endings between their papillae, indicating that the higher number of papillae-associated endings in these animals was not merely due to changes in papillae size. No significant differences were found for ending densities outside the papillae region (from beginning and end of the pad to the first papilla) or over the entire pad. Epidermal ending densities were calculated by dividing the number of endings in a region by its length. (H) Both *Bbs* mutants had significantly longer papillae widths but not heights. Papilla height was measured from its estimated base to its peak height in the epidermis, and width was calculated by dividing the area of the papilla by its height. dp, dermal papilla; sg, sweat gland; e, epidermis; d, dermis.

induction of the immediate early gene *c-Fos* in second-order sensory neurons of the spinal cord dorsal horn (20). A reduction of thermally induced *c-Fos* in the dorsal horn, as measured by counting the number of *c-Fos*-positive nuclei, would indicate that a defect at least occurs in the peripheral innervation or the activation of the second-order neurons. If *c-Fos* induction remains normal in the dorsal horn, then the defect may be occurring at higher CNS processing centers (20). We stimulated one paw of three mutants and three WT littermates at either 48°C or 52°C and quantified nuclear *c-Fos* expression on the ipsilateral dorsal horn across serial sections of the lumbar region (L3–L5), blinded to the genotype. In contrast to robust activation of dorsal horn neurons in WT animals exposed to a 48°C stimulus, we observed little or no activation of *c-Fos* in *Bbs1* mutants' dorsal horn neurons at the same temperature (Fig. 2 C and D). The response of mutants and WT animals remained significantly different at 52°C, although at this temperature, the mutants demonstrate some responsiveness, further suggesting the presence of a peripheral sensory anomaly.

Anatomical Defects in s.c. Innervation in BBS Mutant Mice. To determine whether changes in peripheral innervation might contribute to the observed sensory deficits, we analyzed glabrous hind paw (GHP) skin sections immunolabeled for PGP 9.5, a panneuronal marker, and CGRP, a marker of peptidergic innervation (Fig. 3; SI Table 2). Qualitative analysis revealed reductions in CGRP immunoreactivity (IR) among fibers within dermal papillae of both *Bbs* mutants (Fig. 3 A and B). Meissner corpuscles, which normally express low levels of CGRP-IR (21), were not noticeably affected. The distribution of sensory endings within the epidermis and the size of dermal papillae were also altered in both *Bbs* mutants. In WT pads, innervation has a relatively uniform distribution throughout the epidermis whereas in *Bbs* mutants, it is disproportionately concentrated at dermal papillae (Fig. 3C). Quantification conducted on GHP tissue labeled for PGP 9.5 and mouse anti-Cy2 to delineate the dermal–epidermal border confirmed that both *Bbs* mutants had increased sensory endings above and at the border of their papillae, which were also wider than WT (Fig. 3 F and H). The

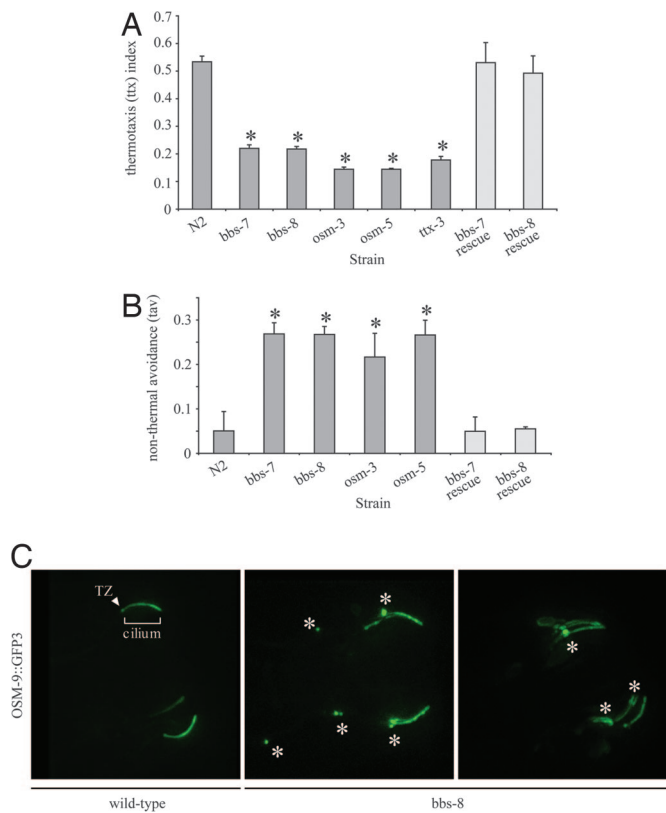


Fig. 4. *C. elegans* ciliary mutants show thermotaxis and thermal avoidance defects as well as mislocalized OSM-9. (A) Thermotaxis and thermal avoidance of WT (N2), *bbs* mutants, and *osm-3* kinesin mutants. Thermotaxis relates to how well the worms move to their rearing temperature zone (20°C). (B) Nonthermal avoidance is the proportion of worms that do not avoid a noxious temperature presented near the head of the animal. For A and B, *, $P < 0.00001$. (C) GFP-tagged OSM-9 mislocalizes in *bbs-8* mutant animals. TZ, transition zone/basal body; *, abnormal accumulations not seen in wild-type animals.

overall epidermal ending density across the entire pad was not significantly changed in either of the *Bbs* mutants.

***C. elegans bbs* Mutants Are Thermosensory-Defective.** Although our mammalian data established the thermodeficient phenotypes for our mutants, mammalian innervation is inherently complex, and sensory phenotypes can be variable. Moreover, mammalian sensory neurons also have complex interactions with other cell types that are also ciliated, such as Schwann cells and keratinocytes (22, 23). For these reasons, we turned to a simpler ciliated organism, *C. elegans*, where we could investigate the consequences of basal body/ciliary dysfunction in thermosensory response exclusively in ciliated sensory neurons.

To test the possible role of *C. elegans* BBS proteins in thermosensation, we first compared the behavior of two previously described *bbs* mutants (14), *bbs-7* (also known as *osm-12*) and *bbs-8*, with that of their WT counterparts in a thermotaxis assay (24). When placed on a shallow linear thermal gradient ranging from 18.5°C to 21.5°C (across 8 cm), WT animals moved effectively to their rearing temperature of 20°C over a period of 1 h (Fig. 4A). By contrast, *bbs-7* and *bbs-8* mutants displayed statistically significant defects ($P < 0.00001$) in their thermotaxis to the 20°C zone (Fig. 4A). An equal number of thermotaxis assays were performed by placing the animals on the hot or cold side of the agar slab, and the results implied that ciliary mutants were defective in general thermosensation, showing no preference for warm or cold temperatures. This phenotype cannot be

ascribed to locomotory defects, because the mutant animals display movement (i.e., bends per minute) indistinguishable from WT (data not shown). In addition, *bbs-7* and *bbs-8* mutant strains rescued with their respective WT genes showed restored thermotaxis behaviors (Fig. 4A; *bbs-7* rescue = 0.5307 ± 0.073 ; *bbs-8* rescue = 0.4925 ± 0.063). Importantly, these defects were not restricted to the *bbs* mutants, because other ciliary mutants, including *osm-5*, which encodes the ortholog of IFT52 (25), and *osm-3*, which encodes the homodimeric kinesin required for building the distal segment of *C. elegans* cilia (26), also displayed thermotaxis defects ($P < 0.00001$) that were comparable with those of *bbs* mutants (Fig. 4A). Also of interest, the general morphology of the microvilli-decorated AFD thermosensory neuron cilium was intact, suggesting that only defects in the underlying cilium caused the phenotype (data not shown).

Next, to test whether thermosensory defects extend to noxious temperatures, we performed a thermal avoidance assay, in which the response of individual worms to a nociceptive temperature ($\approx 50^\circ\text{C}$) placed directly in the path of their movement near their head was measured (27). WT animals ($n > 400$) stop their forward movement and initiate a distinct, reproducible reflexive reversal in 94.9% of the cases (Fig. 4B; see also ref. 27.). By contrast, *bbs-7* and *bbs-8* mutants ($n > 400$) both showed poor avoidance phenotypes ($P < 0.00001$), with proper avoidance responses observed in only 73.1% and 73.3% of the cases, respectively. Similarly, the *osm-3* and *osm-5* mutants displayed avoidance in 78.3% and 73.4% of the cases ($P < 0.00001$), respectively (Fig. 4A). To ensure that the thermal deficient phenotypes are specifically due to mutations in *bbs*, we confirmed that *bbs-7* and *bbs-8* mutants expressing their WT transgenes had thermal avoidance responses comparable with that of WT animals (*bbs-7* rescue = $95.0\% \pm 3.2\%$; *bbs-8* rescue = $94.5\% \pm 0.4\%$; Fig. 4B).

We next sought to probe further the biochemical basis of this phenotype. One possibility was that defective ciliary function might perturb the movement of effector molecules, of which TRP receptors would represent ideal candidates. We therefore examined the movement of OSM-9 in our mutants. Because no *C. elegans* TRP channel has yet been linked specifically to thermosensation, we focused on OSM-9, a known axonemal protein that is required for chemotaxis and represents a potential functional homolog of mammalian TRPV1 or TRPV4 (28, 29). We found that a GFP-tagged version of OSM-9, which localizes properly to the ciliary axoneme in WT animals, shows variable but consistent mislocalization in a *bbs* mutant background. Specifically, *bbs-8* animals display accumulations/mislocalization not seen in the WT animals or in *bbs-8* rescue animals, along the dendrite, within or in proximity to the basal body, and along the ciliary axoneme (Fig. 4C). Although OSM-9 is not the *C. elegans* thermosensory receptor *per se*, our findings suggest that at least one molecular explanation for the thermosensory phenotype is that a cilium-based thermosensory apparatus (e.g., TRP-type receptor) mislocalizes or is not functional when BBS protein function is disrupted.

Defective Receptor Distribution in Murine DRG Neurons. Even though the anatomy of the *C. elegans* sensory neuron is markedly different from that of peripheral sensory neurons in mammals (not least because of the position of the cilium relative to the site of sensory input), our data raised the distinct possibility that mistrafficking or misregulation of thermo- and mechanosensory channel proteins might contribute to the observed phenotypes in the mouse. To examine this possibility, we focused on the mammalian TRPV1 receptor, activated at the range where the phenotype was primarily observed (30) and STOML3, a stomatin-like protein that has been shown recently to be necessary for mechanosensation (31), and which we have found previously to be mislocalized in the olfactory epithelium of BBS mouse mutants (5).

We first evaluated the distribution of TRPV1 in GHP sections from each of our mutants and WT littermates. We did not observe

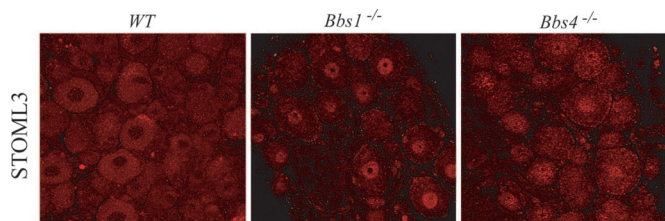


Fig. 5. Distribution of STOML3 in DRG neurons. In contrast to WT animals, STOML3 staining is perturbed in BBS mutants, where it appears to be mistrafficked to the nucleus. Images are at magnification, $\times 40$.

any noticeable staining differences among the endings (data not shown). However, when testing another compartment of these neurons, we did observe altered TRPV1 immunoreactivity at the soma as determined by blinded scoring of consecutive sections across the DRG. Four of six *Bbs1*^{-/-} animals had depressed TRPV1 signal as judged by the average intensity of positively stained neurons, whereas the *Bbs4*^{-/-} animals exhibited an increase in intensity of TRPV1-positive somata (SI Fig. 8*A* and *B*). This was reminiscent of previously observed defects of olfactory neurons, where *Bbs1*^{-/-} and *Bbs4*^{-/-} animals exhibited antithetical cellular phenotypes, both of which culminated in the same functional defect (32). We do not know whether this finding reflects abnormal neuronal specification (potentially as a consequence of a defective cilium) or whether the trafficking of the receptor is perturbed.

We found similar disturbances in the distribution of STOML3; whereas modest amounts were detected in the cytoplasm (and possibly the plasma membrane) of cells in sections across the DRG in WT animals, we observed pronounced STOML3 accumulation in the nuclei of both *Bbs1*^{-/-} and *Bbs4*^{-/-} animals (Fig. 5), a distribution predictive of a mechanosensory defect.

Sensory Defects in BBS Patients. The establishment of defective thermosensory/nociceptive responses in basal body and ciliary mutants in mouse and *C. elegans* raised the distinct possibility that BBS patients might also exhibit hitherto unknown sensory deficiencies. To test this hypothesis directly, we recruited nine unrelated BBS patients over the age of 17 and, upon informed consent, assayed them for seven sensory modalities using standard neurological testing. All patients had a noticeable diminution in their ability to detect vibration when the fork was applied to the medial and lateral condyles at the dorsum of the wrist and each displayed poor two-point discrimination over the palm and dorsum of the hand. Seven of the nine (78%) had diminished proprioception (joint position sense), four of nine (44%) had diminished temperature sensitivity, and seven of nine (78%) were unable to accurately define the weight or shape of the object placed in the palm (Table 1).

Discussion

Here, we have shown that the somata of mammalian sensory neurons are ciliated and that loss-of-function mutations in ciliary and basal body proteins affect the function of these cells, which translate to defects in the perception of thermosensation in the mouse, and broad sensory phenotypes in humans. To our knowledge, this association in mammals between basal body/ciliary proteins and thermosensation is previously unreported and has potentially significant implications for our understanding of the development and function of peripheral sensory neurons.

Although the precise cellular basis of this phenotype will require further investigation, our data suggest that perturbation of the basal body can possibly lead to concomitant mislocalization of TRPV1 and STOML3 in dorsal root ganglia, hinting that defective trafficking, expression, or cellular localization of these channel proteins, or indeed neuronal specification, might contribute to the observed phenotypes. Our finding that *C. elegans* OSM-9 partially mislocalizes in *bbs* mutants supports this hypothesis. Also consistent with the transport model, recent data have suggested that PKD2 heterodimerizes with at least one of the thermoTRP channels, TRPV4, and appears to be required for its correct function (M. Kötgen and G. Walz, personal communication), offering a mechanistic link between ciliary proteins and thermosensory deficits. However, additional morphogenetic defects might also contribute, as evident by the aberrant cutaneous innervation of all of the ciliopathy mutants examined. Receptors such as SSTR3 and 5-HT6 have been localized to neuronal primary cilia in the brain (33, 34), and although they have not yet been demonstrated in DRG cilia, SSTR3 mRNA is expressed in DRG cells (35). It is also notable that some neurotransmitters and neuropeptides are thought to be released from the DRG soma (36, 37). Taken together, these observations lead us to speculate that DRG cilia might be involved in sensing key developmental factors, which could in turn regulate the localization and function of peripheral sensory innervation.

At the same time, it is possible that ciliary dysfunction on nonneuronal cells in the periphery may contribute to these changes in innervation. For instance, keratinocytes are known to be ciliated (22), as are Schwann cells (23). A combination of ciliary defects in each of these cell types could therefore contribute to our observed thermosensory and mechanosensory phenotypes; conditional ablation of ciliary proteins in sensory neurons, discrete keratinocyte layers and glial cells as well as adult-specific mutants will thus be required to dissect the relative spatiotemporal contribution of each tissue.

Finally, our BBS patient data suggest that perturbation of peripheral sensory neurons might not be restricted to thermosensation but might also hold true for other modalities. It will be important to determine the extent and nature of these defects and whether they are restricted to the skin. In parallel, it is paramount to determine whether such phenotypes are present in other ciliary syndromes. Recent work has highlighted the cil-

Table 1. Sensory phenotypes in unrelated BBS patients

| ID | Sex | Age, y | Light touch | Pain | Vibration | Proprioception | Temperature | Two-point discrimination | Weight/shape recognition |
|-------|-----|--------|-------------|------|-----------|----------------|-------------|--------------------------|--------------------------|
| 227.1 | F | 17 | + | ↓ | ↓ | + | + | ↓ | ↓ |
| 128.2 | M | 20 | + | + | ↓ | ↓ | + | ↓ | ↓ |
| 128.1 | F | 18 | + | + | ↓ | ↓ | ↓ | ↓ | ↓ |
| 181.1 | M | 18 | + | + | ↓ | + | + | ↓ | + |
| 012.1 | M | 24 | ↓ | ↓ | ↓ | ↓ | ↓ | ↓ | ↓ |
| 012.2 | M | 26 | + | + | ↓ | ↓ | + | ↓ | ↓ |
| 012.3 | M | 20 | + | ↓ | ↓ | ↓ | + | ↓ | + |
| NK1.1 | M | 32 | + | ↓ | ↓ | ↓ | ↓ | ↓ | ↓ |
| NK1.2 | M | 29 | ↓ | ↓ | ↓ | ↓ | ↓ | ↓ | ↓ |

+, normal sensory response; ↓, reduced sensory response.

